

Semiconductor–metal phase transition induced in InSb by a strong electromagnetic field

G. G. Gromov, V. V. Kapaev, Yu. V. Kopaev, and K. V. Rudenko

P. N. Lebedev Physics Institute, USSR Academy of Sciences

(Submitted 11 May 1988)

Zh. Eksp. Teor. Fiz. **94**, 101–113 (December 1988)

It is found by experiment that strong electromagnetic (laser) radiation produces in InSb at low temperatures (77–190 K) a phase transition with formation of a metallic phase. This transition proceeds via an intermediate state characterized by production of a wurtzite phase. Since metallic phase is metastable under normal conditions, its properties can be determined and suggest that it has a β -Sn structure. A theoretical model points to an electron-stimulated mechanism for the phase transition. It is shown that the onset of excitation inhomogeneities can explain why the nonequilibrium carrier densities N_{cr} needed for the phase transition are obtained even though the average density satisfies $N_{av} < N_{cr}$. It is established that ordering of the excitation inhomogeneities, meaning a transition to a periodic structure, permits the phase transition to continue until a continuous layer of the new phase is formed. The diffractive redistribution of the radiation flux over the surface is such that it stimulates the phase transition.

The possibility of nonequilibrium phase transitions, electron-stimulated in semiconductors by strong electromagnetic (laser) radiation, was predicted theoretically.^{1,2} It was shown in Ref. 2, for the cases of Si and GaAs, that if the excitations (the nonequilibrium carriers) generated by the radiation have densities $N \gtrsim 10^{21} \text{ cm}^{-3}$ the more closely packed nonequilibrium (metallic) phases become energetically favored over the initial structure.

Electron-stimulated phase transitions are of interest in view of the problem of mechanisms for semiconductor annealing by lasers, currently receiving considerable attention.^{3,4} It is known that the metal phases of most class IV semiconductors and III-IV compounds, usually used in laser experiments, exist only at high pressures.⁵ Drawing the analogy between nonequilibrium carriers and the influence of pressure, it can be noted that electron-stimulated phase transitions can be observed only under conditions of laser dynamics, and large nonequilibrium-carrier densities are attainable in short laser pulses. This makes the task of observing laser-induced nonequilibrium phase transitions quite complicated, since the results of many high-time resolution investigation procedures are at present difficult to obtain and to interpret unambiguously, even for the already routine tasks of heating and melting by laser pulses.⁴

At the same time, another approach is possible for certain semiconductors with nonequilibrium phases that are metastable under normal conditions. These include antimonide (InSb), whose parameters^{6,7} are close to those of metallic (high-pressure) phases in which a structure, say of the β -Sn type, can be made metastable by fast quenching ($T_q < 210 \text{ K}$).⁸ This dictated the choice of indium antimonide for our investigations. Fast quenching was produced, in analogy with high pressure, by laser irradiation of the sample at low temperatures.

PROCEDURE

The electromagnetic-radiation source was a YAG:Nd³⁺ laser emitting at $\lambda = 1.064 \mu\text{m}$ with pulse duration $\tau = 10 \text{ ns}$. The samples were single-crystal InSb plates

350–400 μm thick with crystal orientation (110), (211), and (111). The sample surface had a class-14 finish obtained by chemical and mechanical polishing. We used also polycrystalline InSb films (500–1000 Å thick) thermally sputtered in vacuum on high-resistance Si substrates. The samples chosen for irradiation were placed in liquid nitrogen or kept in a thermostat at $T = 77\text{--}323 \text{ K}$.

The principal procedure used to monitor the laser action was measurement of the reflection coefficient $R(\lambda = 0.6328 \mu\text{m})$ of the irradiated surface after the passage of a radiation pulse; the accuracy of the procedure was 0.5% (δR). The laser beam covered sample-surface regions of 1–4 mm diameter, and the deviations from uniform surface-energy distribution were at most 5–8%. The He–Ne laser probing-beam diameter was less than 0.1 mm. The irradiated-surface optical constants (the refractive index n and the absorption coefficient k) were measured by laser ($\lambda = 0.6328 \mu\text{m}$) ellipsometry. The measurement results were reduced using a simple one-layer model. The electro-physical properties of the irradiated InSb were determined by measuring the electric conductivity (by a four-point method). To exclude the shunting effect of the conducting substrate, the measurements were performed on InSb films sputtered on high-resistance Si substrates ($\Omega = 1.5 \cdot 10^{-5} \Omega \cdot \text{cm}$).

A combination of methods was used for the physico-chemical measurements of the irradiated sample. The surface topography was investigated by raster electron microscopy (with an S-800 microscope) and by high-depth-resolution profilometry (TALYSTEP profilometer). The chemical composition and the element-distribution profile were investigated by Auger electron spectroscopy using layer-by-layer ion (Ar^+) surface etching (PHI-551 Auger electron spectroscope). Structure investigations were made by transmission electron diffraction (EG-100, 100 kW) and by x-ray structure analysis (using the Debye method) with glancing incidence of the beam ($\text{Cu}, \text{K}_\alpha$); a thermostat maintained the sample temperature constant at 77K.

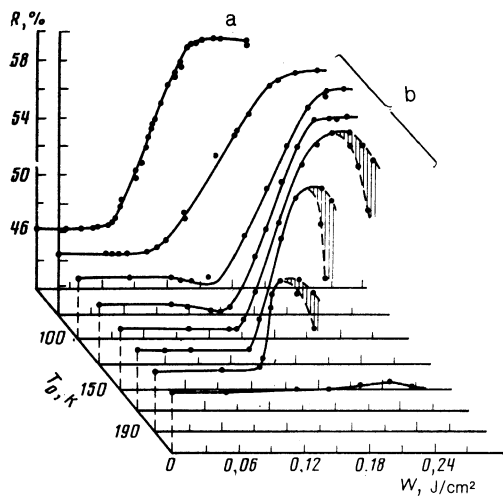


FIG. 1. Surface reflection coefficient vs radiation pulse energy; a—in liquid nitrogen, b—at initial temperatures T_0 .

RESULTS

Irradiation of samples immersed in liquid nitrogen caused an appreciable increase of the surface reflection coefficient, to $R \approx 60\%$ (against the initial $R_0 = 46.2\%$). The plot of R against the pulse energy W (Fig. 1) shows clearly that the onset of the highly reflecting phase has a threshold of $W_{thr} = 0.06 \text{ J/cm}^2$. After rising, the $R(W)$ dependence saturates. Formation of a highly reflecting phase was observed also in laser-irradiated samples thermostatically controlled at $T = 77\text{--}190 \text{ K}$. The character of the dependence of R on W changes gradually as T is raised (Fig. 1b). The threshold for the formation of the highly reflecting phase rises to 0.1 J/cm^2 , and the rising part of the $R(W)$ plot becomes steeper. In the interval $150\text{--}190 \text{ K}$ abrupt decreases of R from pulse to pulse are observed for larger W (i.e., the production of the highly reflecting phase is unstable; see the

shaded regions of Fig. 1b), and no increase of R is observed for $T > 190 \text{ K}$.

Ellipsometry of the highly reflecting phase (of a batch of samples) yielded its optical constants ($n = 3.8 \pm 0.1$, $k = 3.25 \pm 0.15$). Comparison of the obtained values with the properties of the initial InSb surface ($n_0 = 4.44$, $k_0 = 1.85$) shows that the increase of R is due mainly to the substantial growth of the absorptivity of the irradiated surface.

Formation of a highly-reflecting phase in single-crystal samples results only from the action of a series of pulses ($i > 1$). The variation of R as a function of i (discrete scale) for different W and T has a distinctive form (Fig. 2), namely, the formation of the highly reflecting phase is always preceded by a surface state with R lower than the initial R_0 . The difference $\Delta R = R_0 - R$ appears only at low temperatures ($\Delta R = 2\text{--}4\%$ for $T = 77 \text{ K}$), and decreases with rise of temperature ($\Delta R \approx 0$ for $T > 250 \text{ K}$). It would be natural to assume that the decrease of R is due to surface damage, as well as to the known formation of a periodic structure³; this leads to diffuse scattering of the light or to a redistribution of the reflected-beam to form a diffraction pattern. However, detailed raster-electron-microscope investigations show that the surface remains planar without visible roughness (at a magnification up to $80\,000$).

What is unique is that formation of a state with decreased R is typical of experiments with single crystals. The reflection coefficients of laser-irradiated polycrystalline InSb films jump after the very first pulse to the maximum value corresponding to the given W (Fig. 1), i.e., no stage with formation of a low-reflection state is observed.

Interest attaches to the behavior of the highly reflecting phase after laser irradiation. A gradual decrease of R all the way to R_0 was established. Measurements at $288\text{--}323 \text{ K}$ have revealed a strong temperature dependence of the lifetime on the highly reflecting phase (Fig. 3). The experimental values of the relaxation time τ , for fixed W , plotted with $\ln \tau$, and T^{-1} as coordinates, are well approximated by the rela-

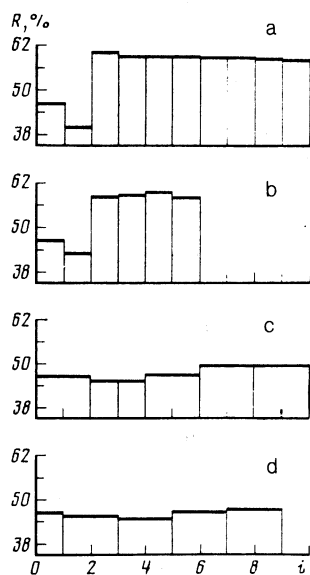


FIG. 2. Reflection coefficient R vs the number of pulses (in liquid nitrogen) for different values of W [J/cm^2]; a—0.16, b—0.12, c—0.08, d—0.064.

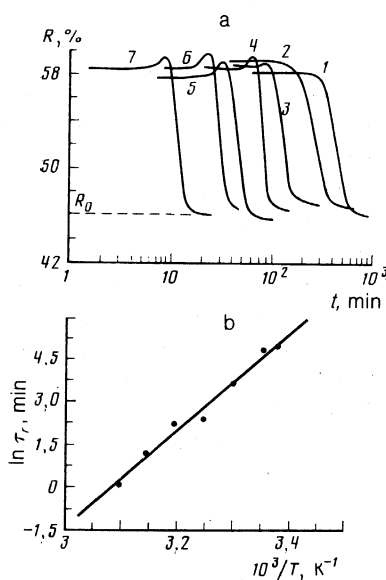


FIG. 3. a—Temperature dependence of the reflection-coefficient relaxation: 1—293 K; 2—298, 3—303, 4—308, 5—313, 6—318 K, 7—323 K; b—plot with coordinates $\ln \tau$ and T^{-1} .

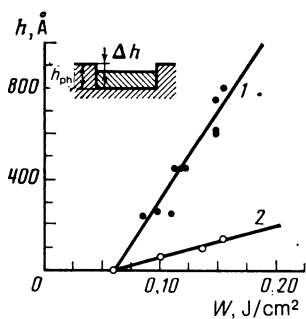


FIG. 4. Results of irradiated-surface profilometry: 1— h_{ph} , 2— Δh .

tion $\ln \tau_r$ [min] = $-52.6 + 1.7 \cdot 10^4 T^{-1}$. The relaxation activation energy is thus $\Delta E_a = 1.48$ eV/molecule.

Combination of the measurement of R with chemical etching of the highly reflecting phase, followed by profilometry of the etched surface, has made it possible to measure the thickness h_{ph} of the produced phase (etching was continued until R decreased to its initial value). This yielded the dependence of h_{ph} on the energy W (Fig. 4, curve 1). The dependence of the thickness of the highly reflecting phase on the experimental conditions is well explained by the character of the curves in Figs. 1 and 3a, where the sections in which the reflection coefficient changes are apparently indicative of a change of the phase film thickness inside the skin layer (δ), when R is insensitive to h_{ph} . Note that the presence of local maxima on R on the relaxation curves (Fig. 3a) is obviously due to interference in the highly reflecting film when its thickness is close to δ and the interference effects made an additional contribution to R .

Profilometry of the InSb surface immediately after the laser action has shown that the irradiated section "caves in" below the initial surface to a depth Δh up to 120–150 Å. The experimental dependence of Δh on W is shown in curve 2 of Fig. 4. Relaxation of the reflection coefficient (Fig. 3a) makes the surface planar. This fact is evidence of a reversible increase of the density in the layer of the product phase ($\rho = \rho_0 h_{ph} / (h_{ph} - \Delta h)$, where ρ_0 is the density of the initial InSb). Putting $\rho_0 = 5.775$ g/cm³ (Ref. 10) and taking the measurement error into account, we obtain $\rho = 7.0 \pm 0.2$ g/cm³.

The results of the profilometry and of the thickness measurement of the highly-conducting-phase film have made it possible to obtain information, by a four-point method, on the resistivity of the new phase. To this end, the measurements were performed on polycrystalline InSb films of known thickness. Using the $h_{ph}(W)$ dependence (Fig. 4, curve 1), a layer of given phase thickness was produced by a laser. The measurements have shown that the resistivity of the highly reflecting phase is substantially lower than that of the initial polycrystalline InSb ($\Omega = 1350 \pm 100 \mu\Omega \cdot \text{cm}$ as against $\Omega_0 = 4100 \pm 300 \mu\Omega \cdot \text{cm}$). After the relaxation of R , the resistivity resumed a value close to the initial one.

The measurement results show thus that action of a nanosecond laser on InSb at low temperature produces a phase transition in the irradiated layer. The next set of experiments was therefore devoted to ascertaining the nature of the observed phase transition, which can in general be due to both structural and chemical changes.

Layer-by-layer Auger-electron spectroscopy (AES) revealed no change in the chemical composition, since the

typical stoichiometric In-to-Sb density ratio ($x_{In}/x_{Sb} = 1$) was preserved. Furthermore, there was no evidence of chemical interactions in the irradiated region or of formation of chemical compounds other than a thin (30–40 Å) layer of natural surface oxide always present on a real InSb surface.⁷ Thus, AES has revealed no noticeable changes whatever capable of explaining the observed formation of a metastable highly reflecting phase. On the other hand, data were obtained on structural changes in irradiated InSb. Transmission electron diffractometry has revealed the presence of a number of reflections that differ from those obtained for the initial indium antimonide with sphalerite structure. The new system of reflections attests to a restructuring of the cubic lattice. The interpretation of the results, however, meets with the basic difficulty that the electron beam causes local heating of the analyzed section.

In view of the strong temperature dependence of the stability of the highly-reflecting phase (Fig. 3), it can be stated that the electron diffraction patterns record not the structure of the metastable phase, but the "history" of its relaxation. An x-ray structural analysis by the Debye method was therefore carried out. The measurements were made at 77 K on polycrystalline InSb films and on single-crystal samples, oriented in the direction of the cleavage planes relative to the x-ray beam. The Debyeograms of the irradiated polycrystalline films had lines with interplanar distances 2.91, 2.82, 2.65, 2.04, and 2.02 Å, in good agreement with the known data on the metallic phases of InSb.^{6–8,11} The relaxation of R is accompanied by vanishing of this group of lines.

The unconventional use of the Debye method to study single-crystal samples was prompted by the need to determine the nature of the low-reflectivity state that set in after the first pulses (Fig. 2). A strong (slightly blurred) reflection was observed, corresponding to an interplanar distance $d_{hkl} = 3.48$ Å, which can be attributed to formation, in the irradiated layer, of a wurtzite phase or of wurtzite stacking faults in the sphalerite lattice. The presence of a strong reflection with $d_{hkl} = 3.48$ Å was recorded also for single-crystal samples after relaxation of the reflection coefficient. Thus, a low-reflectivity state not only precedes the appearance of a highly reflecting phase, but is also formed when the latter relaxes. This is confirmed by the appearance of the negative ΔR typical of the low-reflectivity state when relaxed samples are cooled to 77 K. In addition, no decrease of R (on the i scale) occurs when the relaxed samples are again irradiated by a laser. It should be noted that irradiated polycrystalline films do not go through a stage in which R decreases, i.e., through an intermediate low-reflectivity state, which seems to indicate that a wurtzite phase is already present in the sputtered films; this agrees with known data.¹²

DISCUSSION

The experimental results show that laser irradiation induces in InSb at low temperatures a phase transition from the basic sphalerite structure (InSb I) to a metastable metallic modification via an intermediate state characterized by presence of the wurtzite modification (InSb II). Since, however, the structure parameters of metallic phase differ little, the product phase cannot be exactly identified. This holds also for other properties, such as the density of any of the metallic InSb modifications whose density ρ is in the range 6.9–7.1 g/cm³ (Ref. 13). Yet a comparison of the behavior

features of the product phase with the properties⁸ of a metastable modification of β -Sn type (InSb III) shows a number of similarities. First, good agreement is observed between the results of the quenching required for metastability of InSb III and of the phase observed in our experiment, an agreement needed to achieve a metastable state, since the quenching temperatures are close (210 and 190–210 K, respectively). Furthermore, it is known from Ref. 8 that in the metastable state the InSb III phase is stable for $T < 288$ K, in good correlation with the stability temperature dependence obtained for the metallic phase produced by laser irradiation (Fig. 3b). Note the non-random character of the observed reverse transition from the metastable phase to a state characterized by the presence of the wurtzite modification of indium antimonide. It has already been reported that InSb III does indeed undergo a phase transition into a mixture of the sphalerite and wurtzite modifications.

The relation between the activation energies E_1 and E_2 of the forward and reverse InSb \rightleftharpoons InSb III transitions is $E_1 = E_2 + \delta E_{12}$, where δE_{12} is the energy difference of the respective states. It is known from Ref. 6 that the activation energy for the InSb I \rightarrow InSb III transition under pressure, which proceeds via a homogeneous nucleation mechanism, is $E_1' = 2.0$ eV/atom. In our experiment, however, recognizing that the metallic phase is produced and relaxes in a thin film, it is obviously necessary to consider a case with heterogeneous nucleation, for which the energy barrier should be lower. Using the close analogy⁶ between the transitions InSb \rightarrow InSb III and α -Sn \rightarrow β -Sn and using the known relation $E_1/E_1' = 0.42$ for the latter, we can estimate the phase-transition activation energy for antimony with heterogeneous nucleation to be $E_1 = 0.84$ eV/atom. The foregoing relation between E_1 and E_2 agrees well with the experimental $E_2 = 0.74$ eV/atom (1.48 eV/molecule), in view of the known¹⁴ value $\delta E_{12} = 0.09$ eV/atom (we ignore here the transition to the state with the wurtzite modification InSb II which is close in energy to InSb I).

Attempts are being made at present to use the thermal model,⁴ in view of its popularity, to explain many new experimental results. These include some features of the dynamics of laser action and also features of structural transformations such as amorphization.^{15,16} The nonequilibrium phase transition we have observed does not accord with the well known premises of the thermal model.

According to the latter, structural transformations produced by short laser pulses are based mainly on the dynamics of recrystallization of the radiation-melted surface layer, which is sensitive to W (if $W \gg W_m$) and to τ . This describes well the experimentally observed amorphization. The difference of the initial and boundary conditions of laser action at low temperature from those at ordinary (~ 300 K) temperature should change the crystallization and cooling rates, thereby increasing the amorphization probability. In our present work, however, structure methods revealed no amorphization of InSb irradiated in a low-temperature bath. On the contrary, a new crystalline phase is formed. It is remarkable that even the outward manifestations of the observed effect, such as formation of a highly reflecting phase that is uniform over the irradiated sample differ radically from the unique irradiated-surface morphology observed in the case of laser amorphization.⁴

The experimental regimes (λ , τ , W , T_0) of the laser

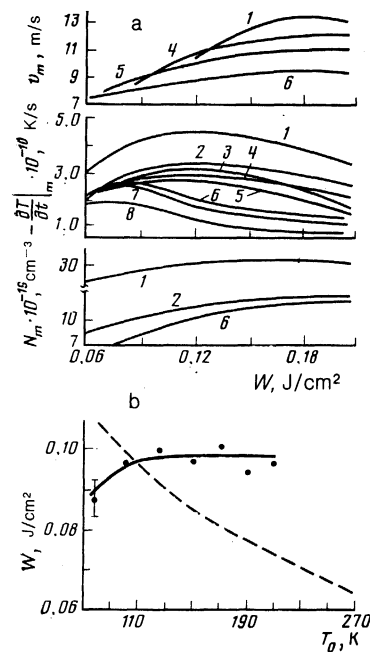


FIG. 5. a—Results, for various temperatures, of numerical simulation of laser action (v_m is the maximum crystallization rate, $\left. \frac{dt}{dt} \right|_m$ the maximum quenching rate in the solid phase, and N_m the maximum density of the nonequilibrium carriers); 1—liquid nitrogen, 2—77 K, 3—100, 4—125, 5—150, 6—175, 7—200, 8—295 K; b— W_{thr} (solid line) and W_{melt} (dashed) vs T_0 .

action on InSb was mathematically simulated to show the role played by the low-temperature conditions. The calculations were based on a simultaneous solution of the heat-conduction and nonequilibrium-carrier diffusion¹⁷ equations, using a numerical procedure developed for the case of heat transfer in liquid nitrogen and under initial conditions $T_0 = 77$ –300 K. The calculation results show that in the general case the maximum crystallization rate v_m increases as the initial temperature decreases from 300 to 77 K (Fig. 5). At the same time, the ranges of v_m for different temperatures are close to one another and overlap, i.e., close crystallization rates are realized under different initial conditions. The formation of the metallic phase, observed only at low temperature, is thus obviously not connected with the increase of v_m as a result of the laser action on the cooled InSb. It must be added that experiment revealed no influence on the sample crystallographic orientation on the main laws governing the formation of the highly reflecting phase (Figs. 1–4), as might be expected in the case of a thermal mechanism.

It is seen from Fig. 5 that at low temperatures, especially in liquid nitrogen, nonequilibrium carriers are generated more effectively. The reason is that at low temperatures the time at which the semiconductor surface layer melts ($W \gg W_{\text{melt}}$), which limits the growth of the maximum carrier density N_m , is delayed by the extra time needed to heat the sample from T_0 to T_{melt} , and in liquid nitrogen also by the heat transfer to the medium.

Note also the dependence, shown in Fig. 5, of the calculated melting threshold W_{melt} on the initial temperature, compared with the analogous dependence for the threshold W_{thr} of formation of a new phase. As seen from Fig. 5, these dependences differ substantially. The value of W_{melt} increases quite strongly with decrease of T_0 , while W_{thr} , on the contrary, decreases, but to a lesser degree. Remarkably, the

calculated melting threshold W_{melt} for InSb in liquid nitrogen is 0.2 l/cm^2 , much higher than the experimental phase-transition threshold at this temperature (Fig. 1a). This is evidence that the detected phase transition occurs in the solid phase prior to the melting.

The results seem thus to supply evidence of implementation of the nonequilibrium-phase-transition mechanism.^{1,2} This pertains primarily to the metallic phase.

Nonequilibrium phase-transition mechanism. A cause, other than heating, of a phase transition into a metallic state, induced in a semiconductor by intense irradiation, is thus the following. When an electron is excited from the valence to the conduction band, i.e., goes over from a bonding to an anti-bonding state, the covalence-bond energy is decreased. The density N of the nonequilibrium electron-hole pairs is determined both by the irradiation intensity and by the carrier lifetime. If the semiconductor in question has a metallic state of close energy or another semiconducting state having a substantially shorter lifetime, the system goes over into one of these states.

The critical density N_{cr} at which such a phase transition should take place was calculated for Si and GaAs in Ref. 2 by means of the pseudopotential method generalized to include a nonequilibrium case. The value of N_{cr} turned out to be $\approx 10^{21} \text{ cm}^{-3}$, with a similar value for indium antimonide. The characteristic feature of such a phase transition was investigated in Refs. 1 and 18 using a Peierls or an excitonic dielectric as a model. In these models one can discern the analogy between the considered transition and the transition of a superconductor into the normal state,¹⁹ but substantial differences are also present. The role of superconducting Cooper pairs in the semiconductor is played here by electron-hole (covalent) pairs.

Comparison of the calculated N_{cr} with the experimental values obtained under typical conditions of laser annealing in silicon and germanium, in the range from nano- to femtoseconds, shows that the experimental value is several times or an order of magnitude lower, than the values necessary for the nonthermal phase-transformation mechanism. A similar situation obtains also under the conditions of our experiments with InSb. Nonetheless, this nonthermal mechanism can take place if the excited electrons and holes tend to "condense." A similar mechanism is known (see Refs. 20 and 21) to produce electron-hole droplets in Si with carrier density $\sim 10^{17} \text{ cm}^{-3}$ at an average density $\sim 10^{12}\text{--}10^{15} \text{ cm}^{-3}$. The cause of this condensation is the correlated interaction of the excitations. Under the present conditions, N is of the order of 10^{20} cm^{-3} and the interaction between the excited carriers can be neglected. At these densities, however, in contrast to the situation with electron-hole droplets, the excitations begin to strongly influence the properties of the crystal itself and to decrease the covalent-bond energy and the bandgap E_g . In the Peierls- and excitonic-dielectric models the decrease of E_g is of the same order as that of the superconducting gap.¹⁹ In addition, just as in superconductivity, an inhomogeneous state sets in,²¹ i.e., the sample contains regions in which the excitation density exceeds the average value and the gap E_g is below average.

This inhomogeneous state is caused by the lowering of the excitation energy of the excitations with increase of their density in some region, due to the decrease of the gap E_g , compensates for the increase of the kinetic energy. The de-

crease of E_g with increase of N can thus play the role of the correlation energy in the problem of an electron-hole fluid.^{20,21}

It is important to note that in the case of a phase transition from one semiconducting phase having a gap E_{g1} to another, likewise semiconducting, with a gap E_{g2} , the main cause of the onset of the inhomogeneous state in the new phase is the difference between the values of the gaps and of the effective carrier masses m_j in these phases. For each of the two phases ($j = 1, 2$) the excitation energy E_j takes the form (we assume for simplicity equal masses of the electrons and holes)

$$E_j = \frac{AN^{3/4}}{m_j} + BNE_{g_j}(0)(1 - \gamma_j N). \quad (1)$$

To determine the optimum density in the region of the onset of the new phase ($j = 2$) it is necessary then to find the minimum difference between the values of E_j for phases 1 and 2:

$$\Delta E = \delta E_{12} + E_2 - E_1, \quad (2)$$

where δE_{12} is the difference between the equilibrium (in the absence of pumping) phase energies. If $E_{g2}(0) < E_{g1}(0)$ and $m_2 < m_1$, a transition to the phase 2 corresponds to an excitation-energy gain due to the decrease of the gap. The lower effective mass, on the other hand, corresponds to an increased kinetic energy of the excitations; at high carrier densities this increase exceeds the energy gain due to the decreased gap. The function $\Delta E(N)$ (Fig. 6, curve 1) has therefore a maximum, just as in the case of an electron-hole fluid. It is this which causes the inhomogeneous formation of phase 2 even when the excitation density N is lower than N_{cr} .

The phase transition observed in InSb, from the semiconducting InSb I (sphalerite phase) to the metallic InSb III with β -Sn structure, proceeds apparently via the intermediate semiconducting phase InSb II (wurtzite structure). It is probable that an inverse situation obtains here, i.e., $E_{g2}(0) > E_{g1}(0)$ and $m_2 > m_1$. At low densities, the transition to the InSb II phase corresponds to an energy loss due to the increased gap. As the carrier density increases, however, the kinetic energy in phase 2 increases more slowly than in phase 1, and the difference ΔE can reverse sign at large N . For inhomogeneous formation of the regions of phase 2 it is necessary that the average excitation density N_{av} exceed the maximum point N_{max} (not to be confused with N_m) on the $\Delta E(N)$ curve (Fig. 6, curve 2). Choosing reasonable limits (not yet determined experimentally) of E_{g2} , m_2 , and γ_2 for the intermediate phase 2 we obtain $N_{\text{max}} \sim 10^{19} \text{ cm}^{-3}$. The increase of the excitation density in phase 2 at $N > N_{\text{max}}$ is limited by the phase transition into the metallic state (phase 3), when the density in these regions reaches the value N_{cr} .

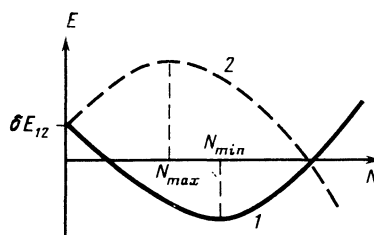


FIG. 6. Dependence of the energy difference ΔE of two states on the excitation density N ; 1— $E_{g2}(0) < E_{g1}(0)$, $m_2 < m_1$; 2— $E_{g2}(0) > E_{g1}(0)$, $m_2 > m_1$.

To identify that part of the sample which goes over into the new phase, it must be borne in mind that the metallic phase is metastable, i.e., it can exist in the absence of excitations.

Besides the above thermodynamic cause of the inhomogeneous state, it must be recognized that the optical properties are independent of N in the considered density range 10^{20} – 10^{21} cm^{-3} . Account must therefore be taken of the electrodynamic origin of a structure with a period on the order of the radiation wavelength.²³

The dependence of the dielectric constant of a semiconductor on the density N of the nonequilibrium electron–hole pairs causes a state that is homogeneous along the sample surface to become unstable in an electromagnetic-radiation field.¹ A periodic distribution $N(x) \propto \cos(2\pi x/d)$ is produced in the surface layer. The period d is determined by the radiation wavelength. At normal incidence we have $d \ll \lambda$ and the wave vector of the structure is directed along the electric vector of the light field.

The locations x_{max} of the density maxima are natural places for the formation of the nonequilibrium metallic state described above. When the critical density is reached in the maxima, a periodic structure is formed and consists of metallic-phase strips on the semiconductor surface. Initially the ratio of the metal interlayer width to the structure period is determined by the ratio of N_{av} to N_{cr} , and does not exceed 0.1 in real experiments.

Since the optical properties of the metal and semiconductor phases differ substantially, the appearance of metal interlayers alters radically the conditions under which the radiation penetrates into the sample. To determine the character of the succeeding evolution of the system we must determine the electrodynamic of laser-radiation diffraction by such a structure.

We solve the problem by using the integral formalism of the exact theory of diffraction.²³ The form of the investigated structure is shown in the inset of Fig. 7. We neglect the deviation of the sample surface from a plane (the height of the relief due to the density differences between the metallic and semiconducting phases is less than $0.02 \mu\text{m}$ in the experiment). We assume that the state of the substance at a surface point having the coordinate x is determined by local values $P(x)$ of the radiation flux through the sample surface. Our problem is thus to calculate $P(x)$ for different metallic-liner widths.

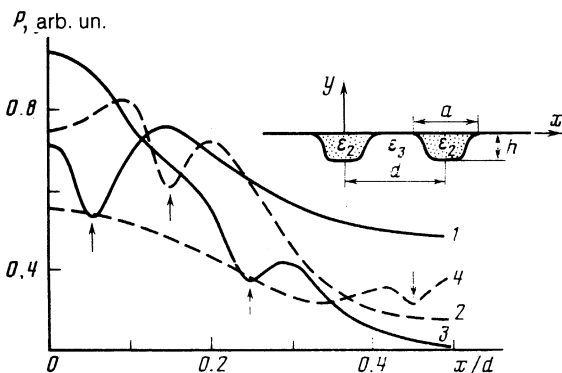


FIG. 7. Radiation-flux distribution along the surface for $\epsilon_2 = -7 + 13i$, $d = 0.98\lambda$, $h = 0.05\lambda$ at different values of a (marked by arrows).

The dielectric constant of semiconducting InSb at $\lambda = 1.06 \mu\text{m}$ is $\epsilon_2 = 1.75 + 2.5i$ (Ref. 5). We do not know the value of ϵ for the metallic phase, but our present measurements yield a reflection coefficient $R = 0.6$. Calculations have therefore been performed for the entire set of ϵ_2 values that yield $R = 0.6$. Figure 7 shows a plot obtained for $\epsilon_2 = -7 + 13i$ ($n_2 = 2 + 3.3i$) and different a ($h = 0.05\lambda$, $d = 0.98\lambda$). In addition, calculations were performed for $\epsilon_2 = -5 + 4.9i$ ($n_2 = 1 + 2.45i$) and $\epsilon_2 = -5 + 22i$ ($n_2 = 3 + 3.7i$). With a and h given, the $P(x)$ plots for various ϵ_2 differ relatively little. For all ϵ_2 , a maximum flux P_{max} is observed in the semiconductor region near the metallic-phase boundary (see, e.g., Fig. 7). The position of the maximum x_{max} and the value of P_{max} for different ϵ do not change by more than several percent. The differences between $P(0)$ and the maxima of P differ somewhat more near the boundary. Since we do not know the exact ϵ_2 , the weak dependence of the results on ϵ gives only a qualitative idea of the role of electrodynamic effects in the evolution of the structure.

The mere presence of a flux maximum near the metal–semiconductor interface can increase the width of the metallic interlayer, since the region where $P(x)$ is a maximum is also the region where the nonequilibrium metallic phase is produced. The value of P_{max} first increases as a function of a , and then decreases. For $a < 0.4d$ the value of P_{max} exceeds the flux $P_{\text{av}} = 1 - R_{\text{av}} = 0.6$ into the homogeneous semiconducting InSb phase. The probability of formation of a nonequilibrium phase in the region of the maximum can be substantially higher than the probability of formation of the initial interlayer. An increase of the interlayer width a alters the value of x_{max} , thereby causing an increase of a . Positive feedback is produced and increases abruptly the width of the metallic strip, from an initial $a_0 = N_{\text{av}}/N_{\text{cr}}$ to $a \approx 0.4$. If the time of nucleation of a new phase is substantially shorter than the laser-pulse duration, this growth will occur within a single pulse, and in the opposite case the metallic strip will increase in width from pulse to pulse.

It is seen from Fig. 7 that the diffractive redistribution of the flux in the structure causes the flux penetrating into the metal to exceed substantially the value $P_m = 1 - R_m = 0.4$ for a homogeneous transition into the metallic state. This leads to additional stabilization of the nonequilibrium magnetic state. Under certain conditions, the increase of the flux into the metal can cause melting. It is thus possible to produce molten regions on a surface at energies lower than the melting threshold. Of importance here is the fact that the melting is preceded by formation of nonequilibrium metallic-state interlayers.

The effects considered by us depend little on the period of the structure, in contrast to the resonant formation of a periodic distribution of $N(x)$ during the initial stage of the processes. The period of the produced metal-strip structure is therefore determined by the period of the $N(x)$ distribution.

Thus, allowance for the flux distribution of the laser radiation diffracted by the evolving structure leads to the conclusion that even if $N_{\text{av}}/N_{\text{cr}} \ll 1$ the restructured sections can cover 50% of the surface when the critical energy corresponding to the density N_{max} is reached (Fig. 6, curve 2). The fraction of the new phase is further increased by an abrupt increase of stimulating-radiation power, and is accompanied by a change of the period of the structure.²⁴ If P_{cr}

is significantly exceeded, the entire series of jumps can be produced within the time of one pulse. Observation of these jumps calls for a high-time resolution investigation of the dynamics of the laser action.

The authors thank V. F. Degtyareva, Yu. O. Mezhennyi, and S. V. Zhuk for help with the experiments.

- ¹V. V. Kopaev, Yu. V. Kopaev, and S. N. Molotkov, *Mikroelektronika* **12**, 499 (1987).
²Yu. V. Kopaev, V. V. Manyailenko, and S. N. Molotkov, *Fiz. Tverd. Tela (Leningrad)* **27**, 3288 (1985) [*Sov. Phys. Solid State* **27**, 1979 (1985)].
³I. B. Khaibullin and L. S. Smirnov, *Fiz. Tekh. Poluprov.* **19**, 569 (1985) [*Sov. Phys. Semicond.* **19**, 353 (1986)].
⁴S. Yu. Karpov, Yu. V. Koval'chuk, and Yu. V. Pogorel'skiĭ, *ibid.* **20**, 1945 (1986) [**20**, 1221 (1986)].
⁵*Landolt-Börnstein Numerical Data and Functional Relationships in Sciences in Technology*, New Ser. Group II, Vol. 17a, ed. by K. H. Hellwege and O. Madelung, Academic, Orlando (1980).
⁶R. E. Hanneman, M. D. Banus, and H. C. Gatos, *J. Phys. Chem. Sol.* **25**, 293 (1984).
⁷S. C. Yu and I. L. Spain, *J. Appl. Phys.* **49**, 4741 (1978).
⁸V. F. Degtyareva, T. I. Belash, and G. V. Chipenko, *Fiz. Tverd. Tela (Leningrad)* **25**, 2968 (1983) [*Sov. Phys. Solid State* **25**, 1712 (1983)].
⁹G. G. Gromov, V. B. Ufimtsev, and K. V. Rudenko, *Poverkhnost'*, No.

12, 80 (1984).

- ¹⁰S. S. Strel'chenko and V. V. Lebedev, *III-V Compounds* [in Russian], Metallurgiya, 1984.
¹¹D. B. McWhan and M. Marezio, *J. Chem. Phys.* **45**, 2508 (1966).
¹²S. A. Semiletov and P. S. Agalarzade, *Kristallografiya* **9**, 490 (1964) [*Sov. Phys. Crystallogr.* **9**, 409 (1964)].
¹³V. I. Petrosyan, O. I. Vasin, and S. I. Stenin, *Pis'ma Zh. Eksp. Teor. Fiz.* **26**, 10 (1977) [*JETP Lett.* **26**, 8 (1977)].
¹⁴J. C. Jamieson, *Science*, **139**, 3557 (1963).
¹⁵E. I. Arutyunov, Yu. V. Koval'chuk, and Yu. V. Pogorel'skiĭ, *Pis'ma Zh. Tekh. Fiz.* **10**, 1281 (1984) [*Sov. J. Tech. Phys. Lett.* **10**, 541 (1984)].
¹⁶A. Yu. Abdulaev, S. V. Govorkov, and N. I. Koroteev, *ibid.* **12**, 1363 (1986) [**12**, 564 (1986)].
¹⁷J. R. Meyer, M. R. Kruer, and F. J. Bartoli, *J. Appl. Phys.* **51**, 5513 (1980).
¹⁸Yu. V. Kopaev, V. V. Menyailenko, and S. I. Molotkov, *Zh. Eksp. Teor. Fiz.* **89**, 1404 (1985) [*Sov. Phys. JETP* **62**, 813 (1985)].
¹⁹V. F. Elesin, and Yu. V. Kopaev, *Usp. Fiz. Nauk* **133**, 259 (1981) [*Sov. Phys. Usp.* **24**, 116 (1981)].
²⁰L. V. Keldysh, *Proc. 9th Internat. Conf. on Physics of Semiconductors*, Leningrad, Nauka, 1968, p. 1307.
²¹S. G. Tikhodeev, *Usp. Fiz. Nauk* **145**, 3 (1985) [*Sov. Phys. Usp.* **28**, 1 (1985)].
²²Yu. V. Kopaev, V. V. Menyailenko, and S. N. Molotkov, *Mikroelektronika* **12**, 222 (1985).
²³R. Petit, *Electromagnetic Theory of Gratings*, Springer, 1980.
²⁴V. V. Kopaev, *Zh. Eksp. Teor. Fiz.* **94**, No. 12, 50 (1988) [this issue, p. 2420].

Translated by J. G. Adashko